JOURNAL OF Applied Polymer SCIENCE

A Novel Water-Soluble, Conducting Polymer Composite for Mild Steel Acid Corrosion Inhibition

A. Ali Fathima Sabirneeza, S. Subhashini
Department of Chemistry, Avinashilingam University for Women, Coimbatore 641043, India
Correspondence to: S. Subhashini (E-mail: subhashini_adu@yahoo.com)

ABSTRACT: A novel water-soluble conducting polymer composite, poly(vinyl alcohol-histidine) was synthesized from aqueous solution by free radical condensation using persulfate. The composite was characterized using UV–Visible, Fourier transform infrared, scanning electron microscopy, thermogravimetric analysis (TG/DTG), and differential scanning calorimetry techniques while its AC conductance was measured by LCZ analyzer. The inhibitive action of the composite on the corrosion behavior of mild steel in 1*M* HCl was studied by conventional weight loss method, potentiodynamic polarization studies (Tafel), linear polarization studies, and electrochemical impedance spectroscopy. The effects of inhibitor concentrations, exposure time, and temperature have been investigated. The corrosion rate, inhibition efficiency (IE), and other parameters have been evaluated for different inhibitor concentrations. The composite provided more than 95% IE at an optimum concentration of 0.6% by weight. The results showed the composite as an effective mixed type inhibitor. The adsorption of this inhibitor obeyed Temkin adsorption isotherm. © 2012 Wiley Periodicals, Inc. J. Appl. Polym. Sci. 000: 000–000, 2012

KEYWORDS: poly(vinyl alcohol-histidine); conducting polymer composite; mild steel; corrosion inhibition; weight loss method; electrochemical techniques

Received 30 June 2011; accepted 27 February 2012; published online
DOI: 10.1002/app.37661

INTRODUCTION

Mild steel (MS) is widely being used for various industrial applications. It is an important material of choice for fabricating various reaction vessels, pipes, tanks, etc., owing to its low cost and high abundance in nature. Despite having these advantages, it experiences series drawback owing to corrosion especially under aggressive environments in processes such as acid pickling, acid cleaning, oil well oxidizing, etc., which results in awful degradation. The rate of degradation is not only affected by the nature of acid but also their concentration and operating temperature. Reports reveal that acid concentrations ranging from dilute to highly concentrated at temperatures in the range of ambient to 130°C cause corrosion of iron.

It has been a perpetual challenge for mankind to preclude the undesired effect of corrosion, particularly in view of the modern-age technological developments. The latest survey by the world corrosion organization shows that the annual worldwide direct loss owing to corrosion is about 1.4 trillion of a nation's GDP value. Early attempts to mitigate the corrosion of metals were empirical and centered largely on the use of organic and metallic coatings. By 1800 itself, inhibitors played a vital role because of the ease in the mode of usage. Most of the effective inhibitors used in industry are organic compounds such as acetylenes, alcohols, ketones, amines, and some nitro compounds.[1–5]

In the 1960s polyacetylic compounds were found to be potential effective corrosion inhibitors.[6] Recently, electro-active conducting polymers such as polyanilines,[7] polyvinylpyridines,[8] and polyamides[9] are being used as corrosion inhibitors for iron/steel, brass, aluminum, and copper.[8–12] However, their usage is deprived owing to difficulty in processing due to their limited solubility in organic solvents and high melting or softening temperatures. Attempts have been made to increase the solubility of polyamides by introducing bulky groups into the polymer backbone.[13,14] In addition, the increasing awareness of health and ecological risks arising from the toxic inhibitors has drawn more attention towards the invention of nontoxic inhibitors which resists corrosion to a maximum, leaving least impact to mankind and nature. The poly(vinyl alcohol)[15] being a water-soluble eco-friendly corrosion inhibitor it was selected for the studies. Here, we report the synthesis of a water-soluble, eco-friendly conducting polymer composite poly(vinyl alcohol-histidine) (PVAH) which can inhibit corrosion of MS to a greater extent.

The present investigation is aimed to study the inhibitive effect of PVAH on MS in 1*M* HCl by weight loss, potentiodynamic polarization, linear polarization, and electrochemical impedance spectroscopy methods. A probable inhibitive mechanism has also been proposed from the viewpoint of adsorption theory.

EXPERIMENTAL

Materials

AR-grade chemicals (Merck, India) and double-distilled water were used for the inhibitor synthesis and for the corrosion inhibition studies. The average chemical composition of the MS used as analyzed by optical emission spectrometry (Baird Spectrovac 1000 Optical Emission Spectrometer) was found to be as follows: (% by weight) Mn-0.196, C-0.106, P-0.027, Cr-0.022, S-0.016, Ni-0.012, Si-0.006, Mo-0.003, and remainder Fe. The mechanically polished MS sheet was cut into strips of dimensions 1 cm × 5 cm × 0.15 cm. The samples were degreased using soap solution and rinsed with trichloroethylene followed by rinsing with double-distilled water. The samples were allowed to dry at room temperature.

Weight Loss Measurements

Weight loss measurements were performed with the dried rectangular strips following the ASTM G31 standard procedure.[16] The strips were immersed in triplicates in 1*M* HCl in the absence and presence of various concentrations of PVAH for different immersion periods at room temperature. At elevated temperatures, a constant immersion period of half an hour was selected and the studies were conducted for various concentrations of PVAH. The strips were taken out and neutralized with $NaHCO_3$. The samples were cleaned to remove corrosion products, dried, and reweighed. From the obtained weight loss, parameters such as corrosion rate (CR),[16] inhibition efficiency (IE_w), and surface coverage (θ) were calculated using the following equations.

$$\mathrm{CR(mpy)} = \frac{3.45 \times 10^6 \times W}{ADt} \tag{1}$$

$$\mathrm{IE}_w(\%) = \frac{W - W_i}{W} \times 100 \tag{2}$$

$$\theta = \frac{W - W_i}{W} \tag{3}$$

where W and W_i are the weight loss (g) of the coupon in the absence and presence of inhibitor, A is the area of the coupon in cm^2, D is the density of the material in g/cm^3, and t is the time of exposure in hours.

Electrochemical Measurements

Frequency Response analyzer (Solartron 1280B) supported with corrware and *z*-plot corrosion softwares was used for data acquisition and analysis. The conventional three-electrode system consisting of saturated calomel electrode (SCE) as reference electrode, platinum foil as counter electrode, and MS strips having exposed area of 1 cm^2 as working electrode was used. The electrodes were immersed in 1*M* HCl solution for 30 min until a steady-state potential was reached. All the tests were performed at 30°C under unstirred conditions without deaeration. The polarization studies were carried out from a potential of +250 to −250 mV (vs. SCE) with respect to the steady-state potential at a scan rate of 2 mV s^{-1}. Anodic and cathodic Tafel segments were extrapolated to obtain corrosion potential (E_{corr}) and corrosion current density (I_{corr}). The IE was evaluated from the measured I_{corr} values using the relationship,

$$\mathrm{IE}_i(\%) = \frac{I^o_{corr} - I_{corr}}{I^o_{corr}} \times 100 \tag{4}$$

where I^o_{corr} and I_{corr} are the corrosion current density in the absence and presence of inhibitor.

The corrware software directly calculates the linear polarization resistance values on the basis of Stern–Geary theory. IE was calculated from the polarization resistance (R_p) values.

$$\mathrm{IE}_{R_p}(\%) = \frac{R_p - R^o_p}{R_p} \times 100 \tag{5}$$

where R^o_p and R_p are the polarization resistance in the absence and presence of inhibitor, respectively.

Electrochemical Impedance measurements were carried out using AC signals of 10 mV amplitude and sweeping the frequency from 20 kHz to 0.1 Hz. The electrode (MS) was kept immersed for 30 min in 1*M* HCl before starting the measurement to attain steady state. The impedance data were analyzed with Zsimpwin software. The charge transfer resistance obtained by fitting the semicircles of the Nyquist representations had been used to calculate inhibition efficiencies of PVAH using the relation,

$$\mathrm{IE}_{R_{ct}}(\%) = \frac{R_{ct} - R^o_{ct}}{R_{ct}} \times 100 \tag{6}$$

where R^o_{ct} and R_{ct} are the charge transfer resistance in the absence and presence of the inhibitor, respectively. The double-layer capacitance was obtained from the maximum value of the imaginary component of the Nyquist plots.

RESULTS AND DISCUSSIONS

Synthesis and Characterization of Water-Soluble PVAH Composite

The inhibitor was synthesized in the laboratory according to the procedure described elsewhere.[17,18] Feed solution consisting of 10% PVA and 1% L-histidine in 0.5*M* oxalic acid was taken in a two-necked flask equipped with thermometer and an addition funnel filled with 1% ammonium persulfate in 0.5*M* oxalic acid. The whole system was kept inside a freezing mixture to maintain the temperature between 0 and 5°C. To the reaction mixture, ammonium persulfate was added in drops with constant stirring using a magnetic stirrer. The reaction mixture was kept under refrigeration for 24 h. PVAH was precipitated using acetone, filtered, washed, and air dried. Histidine was polymerized by persulfate—radical via condensation reaction which was confirmed by the scanning electron microscopy (SEM)-EDX analysis (TSL-AMETEK). The composite was further characterized by UV–Visible (Systronics-2202), FTIR (Bruker-Tensor-27), NMR (Bruker AVIII 500 MHz), TG/DTA, and differential scanning

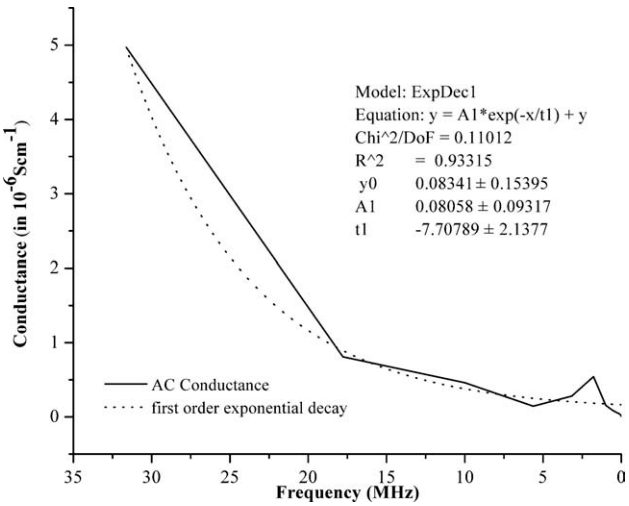

Figure 1. Variation of AC conductance of PVAH with operating frequency.

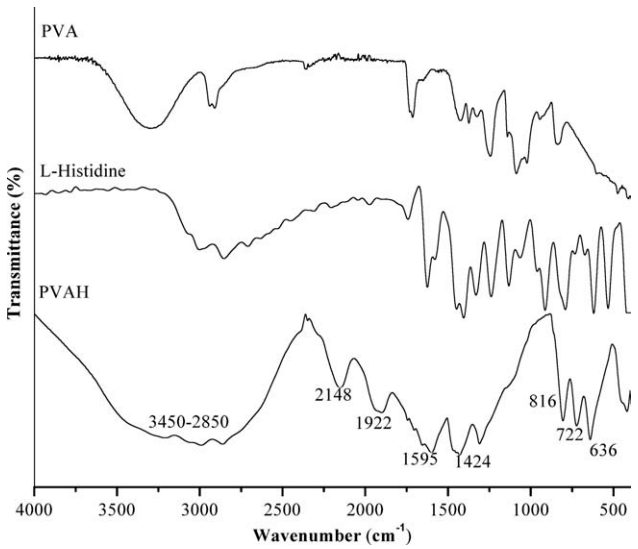

Figure 2. IR spectrum of poly(vinyl alcohol), L-histidine, and PVAH.

calorimetry (DSC) (universal V4.1D TA) analysis. The polymer composite was remarkably soluble in hot water and was also found to be conducting.

The AC conductance of the composite was measured by the LCZ analyzer by varying the frequency from 3 MHz to 300 Hz. The composite was first made into a pellet of diameter 11.03 mm having a thickness of 2.24 mm. The electrical connection was made using silver paste and copper wires. It was found that the conductance of the composite is $\sim$ 1–5 $\times$ 10^{-6} S cm^{-1}, which lies in the range of semiconductors (10^{3}–10^{-8} S cm^{-1}). Figure 1 shows the variation of conductance of the composite with operating frequency and the first-order exponential decay.

UV–Visible spectra of the composite showed two adsorption peaks at 248 and 432 nm which corresponds to n–π^* and π–π^* transitions, respectively. The FTIR spectrum of the polymer composite was analyzed and compared with that of the PVA and L-histidine. The combined FTIR spectrum is shown in Figure 2. PVA showed characteristic peaks for O—H, C—O along with those of C—H vibrations. Spectrum of L-histidine exhibited peaks corresponding to NH_2, COOH, and aromatic —CH— backbone. PVAH showed characteristic peaks for OH, NH stretching, and carbonyl absorption of the amide group. A broad peak appearing in the region 3450–2850 cm^{-1} is owing to the OH stretching of PVA,[19] which is broadened owing to the overlapping of NH stretching bands of polyhistidine and the aromatic C—H stretching vibrations. The peak at 2148 cm^{-1} is associated with the C—N stretch of the polyamide. The amide C=O stretching vibration of polymerized histidine is found at 1595 cm^{-1}. The C—H deformation bands were observed in the region 1420 (PVA backbone) and 900–600 (histidine nuclei) cm^{-1}. The absence of prominent bands of the acid group in the region 1730–1700 cm^{-1} confirms the polymerization of amino acids.

The comparison of NMR spectrum of the composite with the reactants showed a small shift in the values of —CH_2 and —CH protons of poly(vinyl alcohol) and the proton signal of histidine nucleus confirming the formation of the composite. The chemical shift values of PVA, histidine, and PVAH are tabulated in Table I. The shifts in PVAH may be attributed to the hydrogen bonding.

The surface morphology of the composite was studied using SEM (TSL-AMETEK advanced microanalysis system). The SEM image, EDX spectrum, and the elemental composition of complete phase, PVA matrix, and poly-histidine phase are shown in Figure 3. The EDX analysis of the total phases showed about 21 wt % nitrogen and 22 wt % oxygen. Phase 1 (PVA Matrix)

Table I. NMR Chemical Shift Values

Structure	System	Chemical shift (δ ppm)
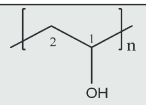	Poly(vinyl alcohol)	*CH(2)—3.64 CH_2(1)—1.65
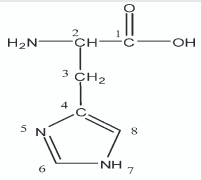	L-histidine	*CH(2)—3.61 CH_2(3)—3.20 CH(6)—7.69 CH(8)—6.89
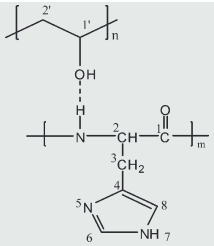	Poly(vinyl alcohol histidine)	#CH(1)—3.87-3.84 CH_2(3)—3.27-3.14, *m* CH(6)—8.56 CH(8)—7.62 CH(1′)—3.95 CH_2(2′)—1.51-1.42

*, Values generated by NMRDB; #, Observed values and $m \ll n$.

Applied Polymer SCIENCE

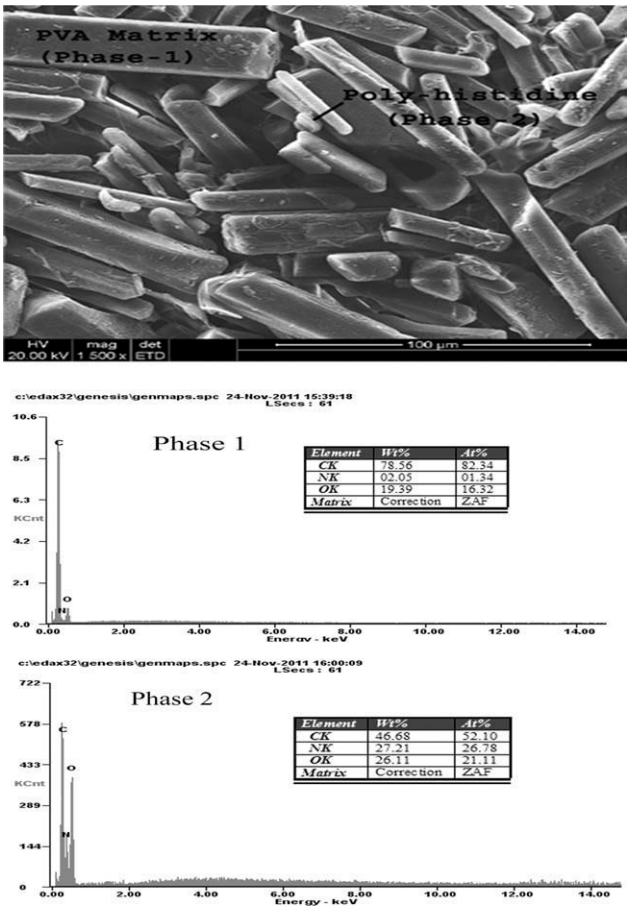

Figure 3. SEM–EDX images of PVAH.

showed only 2 wt % nitrogen, whereas 27 wt % of the Phase 2 (poly-histidine) counts for nitrogen. The presence of high content of nitrogen atom only in the minor phase suggests the simple composite formation. Based on these analyses, the structure of the polymer composite may be proposed as one in which poly histidine chains are randomly distributed in the PVA matrix. The two phases are held together by hydrogen bonds between OH of PVA and NH of the polyamides.

TG/DTG for PVAH and PVA (Figure 4) were carried out in nitrogen atmosphere at a heating rate of 10°C/min with samples weighing ~ 2.5 mg using universal V4.1D TA instruments. The TG/DTG data derived from the experiments are interpreted qualitatively to study the degradation properties of the composite. The thermogravimetry of PVA showed two plateaus around 100°C (removal of moisture) and 283°C (slow degradation of PVA). Exemplary TG/DTG curve of PVAH showed decomposition at 93°C which exorcises the moisture content. The maximum decomposition temperature of PVAH is 247°C which is lower than that of pure PVA (283°C).

The recorded DSC curve for the composite is shown in Figure 5. During the heat treatment of the sample, a change in the trend of the baseline of DSC was observed owing to the elimination of strongly adsorbed water molecules (chemisorbed water through hydrogen bonds). The DSC thermogram of PVA

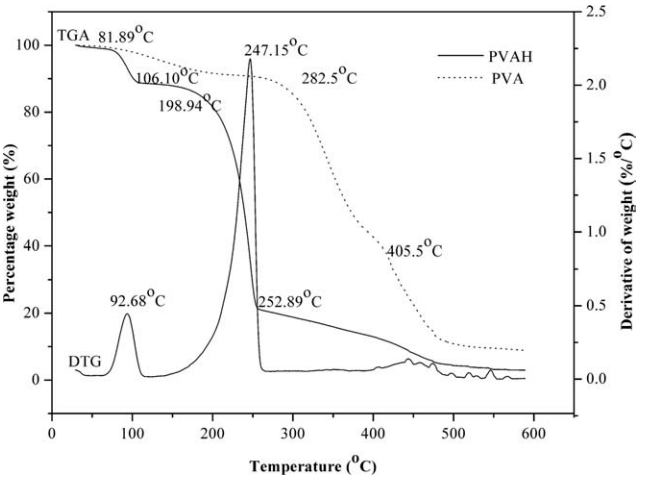

Figure 4. TG/DTG curves of PVA and PVAH.

indicated a glass transition temperature (T_g) of 92°C and a melting isotherm at 292°C,[19] whereas the composite showed glass transition at 99.5°C and melting isotherm at 248°C. As the melting point greatly depends on the purity of the substance, composite showed larger deviation in the melting isotherm.

Weight Loss Method

Effect of Concentration and Immersion Period. In brief, 6% solution of PVAH in deionized water was used as a stock solution for inhibition studies. Weight loss of MS in HCl was determined in the absence and presence of various concentrations (0.06–0.6% by weight) of PVAH. The results were used to calculate IE. Figure 6 shows the variation of IE with concentrations of PVAH. The IE increases with increase in inhibitor concentration up to 0.6%, with further increase in concentration only marginal changes were observed. The increase in IE with the concentration of PVAH is because of the availability of larger number of molecules for adsorption at higher concentrations. No further increase in IE beyond 0.6% of PVAH which is

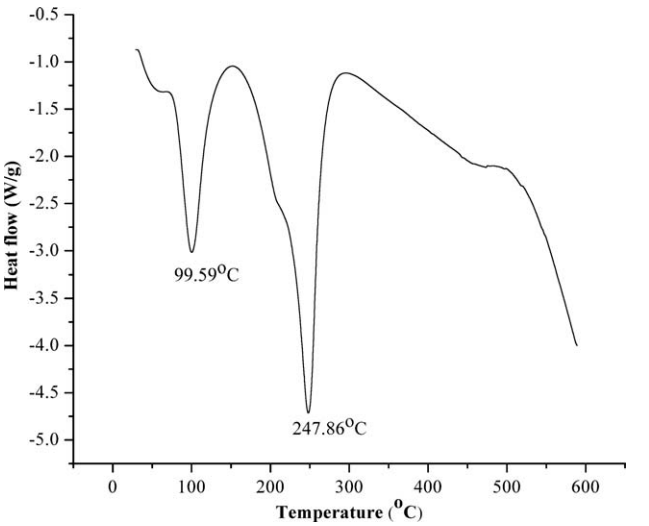

Figure 5. DSC thermogram of PVAH.

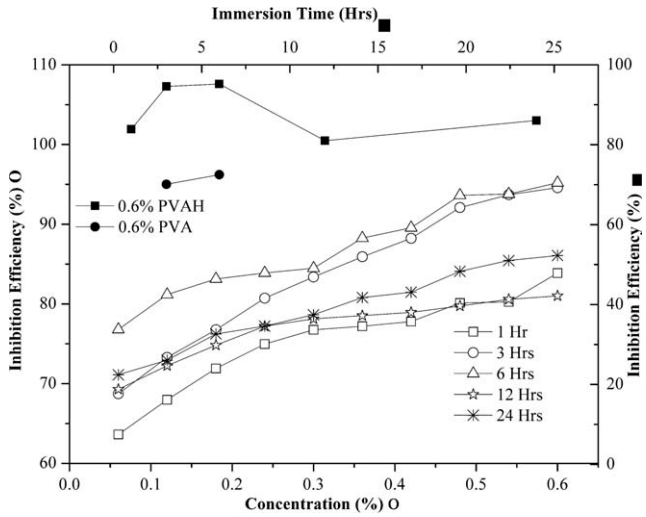

Figure 6. Variation of IE with concentration (○) and immersion time for optimum concentration of PVAH and PVA (●).

attributed to the saturation of adsorption process. It was also found that the IE increases with increase in the immersion time. Figure 6 also includes the inhibition efficiencies obtained for 0.6 wt % of PVA. The results clearly revealed that compositing polyvinyl alcohol with L-histidine increases the IE to 95.19%, which was only 72.5% for PVA at 0.6%. Variation of IE with immersion time for optimum concentration is also shown in Figure 6. It was reported that an adsorbed film is formed on MS surface which is responsible for its corrosion inhibition.[20] The maximum IE (95.19%) was observed for an immersion period of 6 h. At the moment of immersion of MS, concentration of the composite was higher in the medium and hence adsorption proceeds in such a way to attain saturation. The adsorbed layer must be less porous so that it would behave like a barrier, decreasing the CR and thereby increasing the IE.[21] The IE decreases at 12 h of immersion and it seems to increase at 24 h of immersion in 1*M* HCl. This can be attributed to the removal of the adsorbed film owing to the weaker interaction between PVAH and MS surface (physical adsorption). The adsorption of the composite again takes place on the newly exposed surface which results in hike in the IE after 12 h of immersion. Recent article by Fu et al.,[22] reported the corrosion IE of L-histidine as 93.4% at 0.01 mol/L. In this study, 0.0035 mol/L of L-histidine in 0.6% PVAH showed 95% IE.

To establish whether inhibition is owing to the formation of a film on the metal surface via adsorption, scanning electron microcopy was used and the images are shown in Figure 7. It was found that an adsorbed layer is formed on MS surface, which inhibits corrosion. This observation clearly proves that the inhibition is owing to the formation of a film through the process of adsorption of the composite on the metal surface.

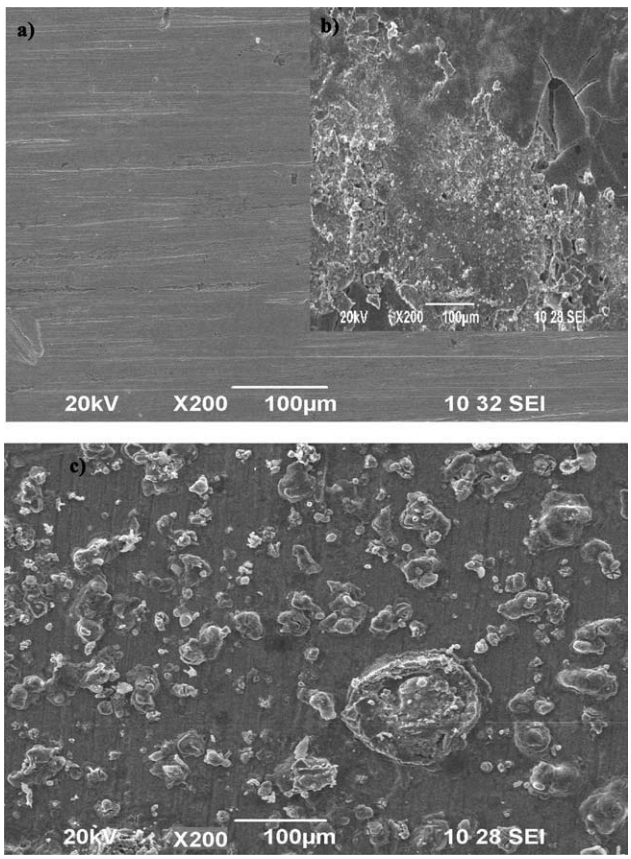

Figure 7. SEM photograph of the MS surface: (a) before immersion; (b) after 6 h of immersion in 1*M* HCl; (c) after 6 h of immersion in 0.6%PVAH + 1*M* HCl at 30°C.

Electrochemical Measurements

Potentiodynamic Polarization Studies. Electrochemical measurements were carried out using Electrochemical Analyzer Solatron-1280 B. The cathodic and anodic polarization curves for MS in 1*M* HCl with varying concentrations of PVAH are shown in Figure 8. Linear polarization measurements and Tafel extrapolation method were used to find the polarization parameters. The values of electrochemical parameters and IE are listed in

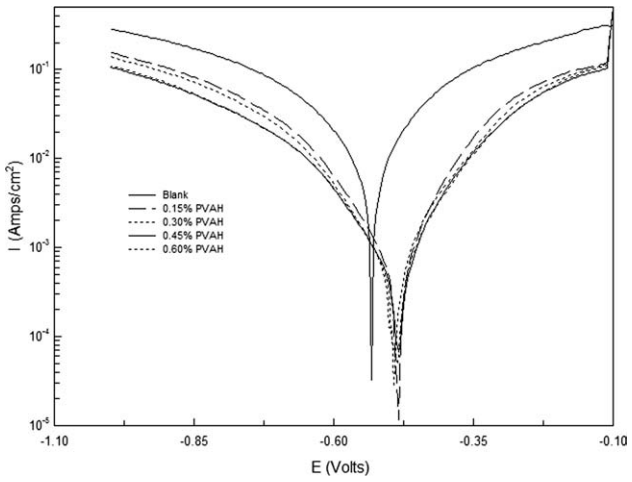

Figure 8. Polarization curves for MS in 1*M* HCl in the absence and presence of different concentrations of PVAH at 30°C.

Table II. Electrochemical Parameters for MS Acid Corrosion in the Absence and Presence of Various Concentrations of PVAH

Conc. of PVAH (%)	Tafel extrapolation method					LPR method		Impedance method		
	b_a (mV/dec)	b_c (mV/dec)	E_{corr} (mV vs. SCE)	I_{corr} (mA/cm^2)	IE_i (%)	R_p (Ω)	IE_{Rp} (%)	C_{dl} (mF)	R_{ct} (Ω)	IE_{Rct} (%)
Blank	128.79	93.94	−527.94	12.87	-	3.30	-	0.4520	9.17	-
0.15	122.17	94.45	−484.13	0.70	94.57	33.87	90.26	0.1573	144.74	93.67
0.30	137.41	104.33	−492.29	0.64	95.04	37.63	91.23	0.1106	169.01	94.57
0.45	118.88	106.13	−484.31	0.63	95.11	40.30	91.81	0.1070	243.94	96.24
0.60	120.82	101.51	−487.37	0.53	95.86	41.49	92.05	0.1093	307.72	97.02

the Table II. These parameters are helpful to predict the nature of the additives—anodic, cathodic, or mixed type inhibitor.

From the results summarized in Table II, it is clear that the values of I_{corr} of MS in the inhibited solution were smaller than those for the inhibitor free solution. The addition of PVAH hindered the acid attack on the MS electrode and a comparison of values in both cases showed that increasing the concentration of the inhibitor gave rise to a consistent decrease in anodic and cathodic current densities, indicating that PVAH act as mixed type inhibitor.[23] There was only a marginal shift in the E_{corr} values which indicates that the additives might have predominantly acted as mixed inhibitor to retard both the rates of cathodic hydrogen evolution and the anodic dissolution of MS. The values of the cathodic and anodic Tafel slopes were also found to change with inhibitor concentrations. This again clearly indicates that the inhibitor controlled both the cathodic and anodic reactions and thus behaved as a mixed type inhibitor.

The current density (I_{corr}) decreases from 12.87 to 0.70 mA/cm^2 with the addition of PVAH (0.6%). The IE was calculated from I_{corr} values[24] and listed in Table I. The maximum IE was found to be 95.86% at 0.6% concentration.

AC Impedance Studies. The corrosion behavior of MS in 1*M* HCl in the absence and presence of various concentrations of PVAH was investigated by electrochemical impedance technique at room temperature. The equivalent circuit model employed for the system was identical to those reported previously in the literature.[25] The measured impedance parameters such as charge transfer resistance (R_{ct}) and double-layer capacitance (C_{dl}), IE, and surface coverage values are provided in Table II. Nyquist Plots for the inhibited and the uninhibited solutions are shown in Figure 9. In the presence of various concentrations of the additives, R_{ct} value increased, whereas C_{dl} value decreased. The charge transfer resistance of the blank was increased from 9.17 to 307.72 Ω on the addition of 0.6% PVAH which results in 97% IE. This suggests that the polymer composite function by means of adsorption at the metal–solution interface.[26] The double-layer capacitance decreased from 0.4520 to 0.1093 mF for 0.6% PVAH. The decrease in C_{dl} values may be owing to the decrease in local dielectric constant and/or increase in the thickness of the double layer.[27] The change in R_{ct} and C_{dl} values was caused by the gradual replacement of the adsorbed water

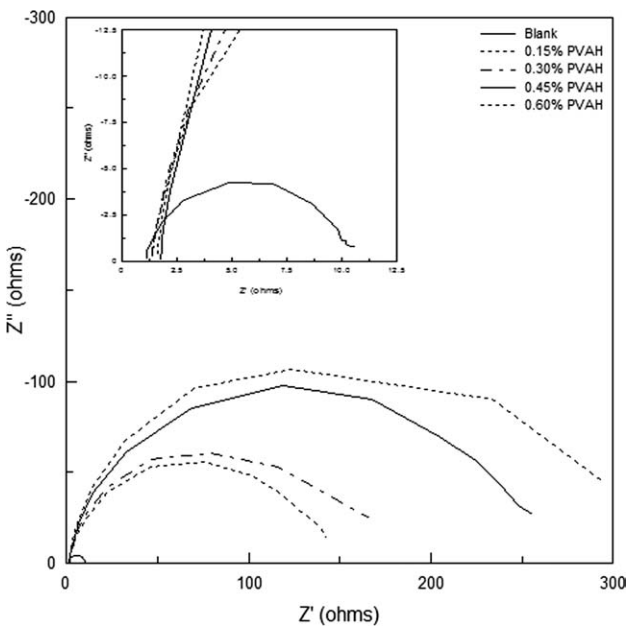

Figure 9. Nyquist plots for MS in 1*M* HCl in the absence and presence of different concentrations of PVAH at 30°C.

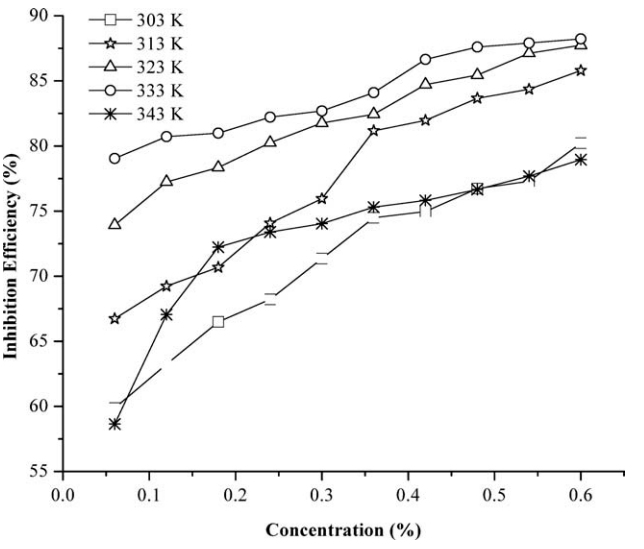

Figure 10. Variation of IE with concentration of PVAH for various temperatures.

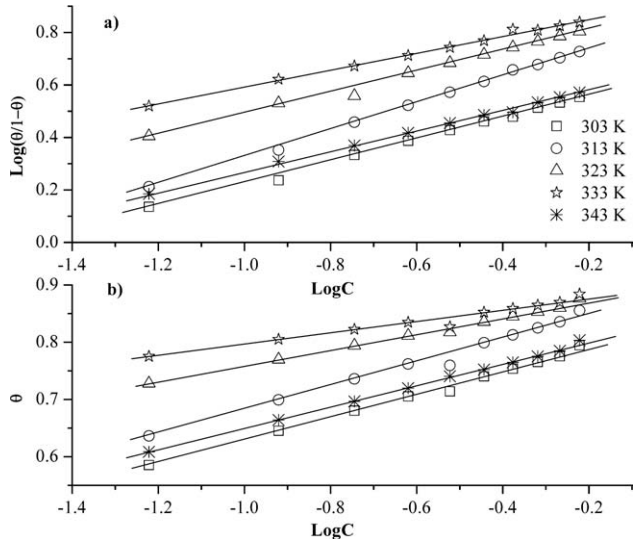

Figure 11. (a) Langmuir adsorption isotherm; (b) Temkin adsorption isotherms.

molecules by the composite on the metal surface.[26] This in total reduces the metal dissolution.

Effect of Temperature

The influence of temperature on the corrosion of MS was studied in the presence of PVAH using weight loss measurement and the results are shown in Figure 10. These studies were used to calculate the activation energy of metal dissolution and free energy of inhibitor adsorption process. The IE was found to increase up to 60°C which indicates the stability of the polymer composite and the adsorbed film at these temperatures. Though at room temperature physical adsorption occurs, at higher temperature some chemical interactions developed between the adsorbed composite and the MS. The maximum IE was found to be 88.24% at 60°C for optimum concentration of PVAH. Though the composite decomposes only above 240°C, there was a drop in IE above 60°C owing to the weak adherence nature of the adsorbed film. Moreover, at higher temperatures the equilibrium shifts in favor of desorption as rate of the desorption process is higher than that of the adsorption at these temperatures.[28]

Adsorption Isotherms. Adsorption isotherms provide information about the interaction of the adsorbed molecules among themselves as well as their interaction with metal surface. The adsorption of inhibitor molecules on the metal surface is the essential step of the inhibition mechanism. The important parameter involved in this is the surface coverage (θ) which can be calculated using weight loss measurements. The θ values for different inhibitor concentrations were tested by fitting to various isotherms.

A plot of Langmuir isotherm (C/θ vs. θ) and Temkin isotherm (θ vs. log C) are shown in Figure 11(a,b). The mean correlation coefficients of the isotherms are 0.9746 and 0.9895 for Langmuir and Temkin, respectively, which are close to unity. This confirms that the present system obeys isotherm models, suggesting monolayer adsorption on the energetically uniform heterogeneous metal surface with interactions in the adsorbed layer.[29]

Kinetic Parameter for Metal Dissolution. The data obtained at the higher temperature studies were used to calculate the activation energy of the systems under consideration. Activation energy (E_a) of the corrosion process was calculated from the Arrhenius equation,

$$\log \mathrm{CR} = -\frac{E_a}{2.303RT} + C \tag{7}$$

where CR is the corrosion rate. Activation energies were calculated from the slopes of the Arrhenius plots (log CR vs. $1/T$) shown in Figure 12 and the results are summarized in Table III. The activation energy was found to increase in the presence of the inhibitor. The activation energy depends on the extent of the surface coverage. The surface coverage and the rate of metal dissolution vary with the concentrations of the composite. It is a general assumption that the corrosion inhibitor greatly enhances the activation energy of the corrosion process.[27] Temperature dependence of the inhibitor efficiency (IE) and the comparison of the values of effective activation energy (E_a) of the corrosion process both in the absence and in the presence of inhibitor lead to some conclusions concerning the mechanism of the inhibiting action. The irregularity observed in the E_a values may be owing to the fact that after a particular stage the actual rate determining step was not the metal dissolution but the metal displacement from the MS surface through the adsorbed layer to the solution.[30] The mean E_a value for corrosion process in the inhibited solution was found to be 54.28 kJ/mol (for blank 43.76).

Thermodynamic Parameters of Adsorption. The change in free energy (ΔG), enthalpy (ΔH), and entropy (ΔS) of the adsorption of the composite on the MS surface in 1M HCl was calculated using the relationships,

$$\Delta G_{\mathrm{ads}} = -RT\ln(55.5K); K = \frac{\theta}{C}(1-\theta) \tag{8}$$

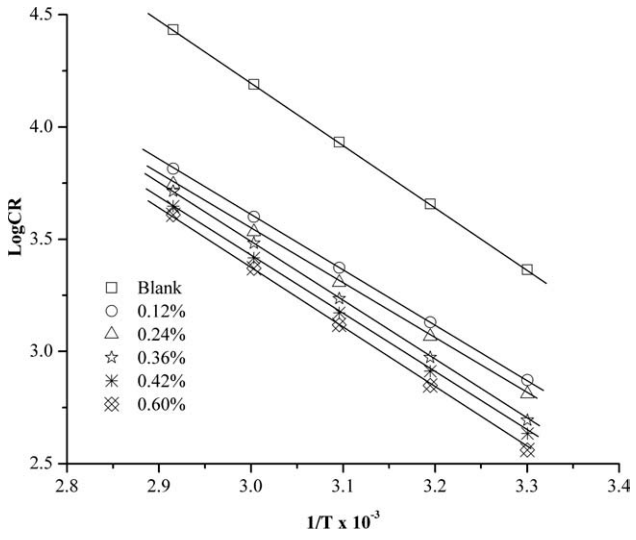

Figure 12. Arrhenius Plot for corrosion of MS in 1M HCl in the presence of PVAH.

Table III. E_a, ΔG_{ads}, ΔH_{ads}, and ΔS_{ads} for MS Corrosion in 1*M* HCl in the Absence and Presence of PVAH

		Free energy of adsorption ΔG_{ads} (kJ/mol)						
PVAH (%)	Ea (kJ/mol)	30°C	40°C	50°C	60°C	70°C	ΔH_{ads} (kJ/mol)	ΔS_{ads} (kJ/Kmol)
Blank	43.76	–	–	–	–	–	–	–
0.06	54.47	18.20	18.79	19.24	23.62	17.68	−7.24	0.038
0.12	52.38	16.81	17.73	17.89	22.11	17.01	−2.88	0.048
0.18	53.29	16.45	17.03	17.26	21.56	16.57	−2.39	0.048
0.24	56.09	16.31	16.65	16.78	21.27	15.91	−5.02	0.038
0.30	54.79	15.79	16.13	16.50	20.75	15.41	−4.49	0.038
0.36	54.12	15.38	15.98	16.11	20.32	15.19	−3.80	0.040
0.42	55.48	15.05	16.18	16.29	19.98	14.87	−5.34	0.034
0.48	56.89	14.96	16.14	16.33	19.84	14.66	−6.40	0.031
0.54	57.05	14.74	16.12	16.39	19.61	14.51	−6.51	0.030
0.60	58.75	14.92	16.05	16.55	19.70	14.44	−7.63	0.027

$$\Delta G_{ads} = \Delta H_{ads} - T\Delta S_{ads} \quad (9)$$

where K_{ads} is the adsorption–desorption equilibrium constant. The calculated values of ΔG_{ads}, ΔH_{ads}, and ΔS_{ads} are listed in Table III. The negative values of ΔG_{ads} indicate the spontaneous adsorption of the composite on the metal surface. The $-\Delta G_{ads}$ values are <40 kJ/mol and confirm physical nature of the adsorption process. The exothermic nature of the adsorption process is indicated by the negative ΔH_{ads} values. The values of ΔS_{ads} are positive, which indicates a decrease in the system order in the presence of additives.[31,32]

Mechanism of Inhibition

Corrosion inhibition of MS in hydrochloric acid medium by different inhibitors (organic, inorganic, and polymers) can be explained on the basis of molecular adsorption. These compounds inhibit corrosion by controlling both anodic and cathodic reactions. In most of the cases, the nitrogen/oxygen atom present in the inhibitor molecules can be easily protonated in acidic solution and converted into quaternary/oxonium ions. These protonated species get adsorbed on the cathodic sites of the MS and decrease the hydrogen evolution and/or to anodic sites through chloride ion interbridge, thereby decreasing the metal dissolution.[33] The adsorption on anodic sites may also occur through the lone pair electrons of the non protonated nitrogen/oxygen atoms which will decrease the anodic dissolution of the MS.[34] The high performance of the inhibitor is attributed to the presence of nitrogen atom, large number of oxygen atoms, larger molecular size, and linearity in the polymeric chain.

CONCLUSIONS

It can be concluded that,

- The composite (PVAH) inhibits the corrosion of MS in 1*M* HCl to a greater extent.
- The high performance of the composite compared to PVA is attributed to the presence of polyhistidine, which acts synergistically.
- The adsorbed film was stable up to 60°C.
- The potentiodynamic polarization revealed the mixed nature of the inhibitor.
- Decrease in double-layer capacitance suggested the increasing adsorption of inhibitor as concentration increases.
- Strong adsorption of the composite molecules on the active sites of the metal surface suppresses the dissolution process and leads to the formation of a protective film.
- The adsorption of the composite follows simple adsorption isotherm.
- The values of free energy of adsorption indicate the spontaneity of the process and its physical nature.

ACKNOWLEDGMENTS

The authors acknowledge Avinashilingam Deemed University for Women, Coimbatore for providing the lab facility and SAIF Center, IIT-Madras for NMR and SEM analysis. One of the authors thanks Council of Scientific & Industrial Research, New Delhi, for providing the fellowship.

REFERENCES

1. Sullivan, D. S.; Strubelt, C. E.; Becker, K. W. High temperature corrosion inhibitors, US Patent **1977**, 7, 4028268.
2. Poling, G. W. *J. Electrochem. Soc.* **1967,** *114*, 1209.
3. Lorenz, W. J.; Mansfeld, F. *Corros. Sci.* **1981,** *21*, 647.
4. Elewady, G. Y.; Mostafa, H. A. *Desalination* **2009,** *247*, 573.
5. Mengoli, G.; Musiani, M. M.; Pagura, C.; Paolucci, F. *Corros. Sci.* **1991,** *32*, 743.
6. I. N. Poutilsva, The chemical and physical changes of inhibitors during the corrosion process, 2nd Eur. Symp. on Corros. Inhib, Ferrara, **1965**, 139.
7. Jeyaprabha, C.; Sathiyanarayanan, S.; Venkatachari, G. *J. Appl. Polym. Sci.* **2006,** *101*, 2144.
8. Abed, Y.; Hammouti, B.; Touhami, F.; Aouniti, A.; Kertit, S.; Mansri, A.; Elkacemi, K. *Bull. Electrochem.* **2001,** *17*, 105.
9. Abdallah, M.; Megahed, H. E.; El-Etre, A. Y.; Obied, M. A.; Mabrouk, E. M. *Bull. Electrochem.* **2004,** *20*, 277.

10. Muralidharan, S.; Phani, K. L. N.; Pitchumani, S.; Ravichandran, S.; Iyer, S. V. K. *J. Electrochem. Soc.* **1995,** *142*, 1478.
11. Umoren, S. A. *J. Appl. Polym. Sci.* **2011,** *119*, 2072.
12. Muller, B.; Triantafillidis, D. *J. Appl. Polym. Sci.* **2001,** *80*, 475.
13. Akutsu, F.; Kataoka, T.; Naruchi, K.; Miura, M.; Nagakubo, K. *Polymer* **1987,** *28*, 1787.
14. Akutsu, F.; Suzuki, A.; Saitoh, F.; Naruchi, K.; Miura, M.; Nagakubo, K. *Makromol. Chem.* **1987,** *188*, 1253.
15. Ebenso, E. E.; Ekpe, U. J.; Umoren, S. A.; Jackson, E.; Abiola, O. K.; Oforka, N. C. *J. Appl. Polym. Sci.* **2006,** *100*, 2889.
16. ASTM G 1–2, Volume-0.3.02, Wear and Erosion; Metal Corrosion, Annual Book of ASTM Standards, ASTM, West Conshohocken, PA, **1996,** 89–95.
17. Ali Fathima, S. A.; Subhashini, S.; Rajalakshmi, R. *Mater. Corros.* **2011,** *62*, 9999.
18. Subhashini, S.; Ali Fathima, S. A. Proceedings WCECS, **2011,** Vol. II.
19. Kunal Pal; Banthia, A. K.; Majumdar, D. K. *AAPS Pharm. Sci. Tech.* **2007, 8** Article 21, doi:10.1208/pt080121.
20. Varsha, S.; Sitashree, B.; Singh, M. M. *J. Appl. Polym. Sci.* **2010,** *116*, 810.
21. El-Etre, A. Y.; Abdallah, M. *Corros. Sci.* **2000,** *42*, 731.
22. Fu, J.; Li, S.; Wang, Y. *J. Mater. Sci.* **2010,** *45*, 6255.
23. Abboud, Y.; Abourriche, A.; Saffaj, T.; Berrada, M.; Charrouf, M.; Bennamara, A.; Hannache, H. *Desalination* **2009,** *237*, 175.
24. Ravichandran, R.; Nanjundan, S.; Rajendran, N. *J. Appl. Electrochem.* **2004,** *34*, 1171.
25. Mansfeld, F.; Kendig, M. W.; Lorenz, W. J. *J Electrochem. Soc.* **1985,** *132*, 290.
26. Quraishi, M. A.; Sardar, R. *J. Appl. Electrochem.* **2003,** *33*, 1163.
27. Mccafferty, E.; Hackermann, N.; Tsai, S. *Corrosion* **1982,** *38*, 57.
28. Wahyuningrum, D.; Achmad, S.; Syah, Y. M.; Buchari; Bundjali, B.; Ariwahjoedi, B. *Int. J. Electrochem. Sci.* **2008,** *3*, 154.
29. Mekki Daouadji, M.; Chelali, N. *J. Appl. Polym. Sci.* **2004,** *91*, 1275.
30. Putilova, I. N.; Balezin, S. A.; Baranik, V. P. Metallic Corrosion Inhibitors; Pergamon Press: Oxford, **1960,** 453.
31. Bouklah, M.; Hammouti, B. *Port Electrochem. Acta* **2006,** *24*, 457.
32. Refaey, S. A. M.; Taha, F.; Abd El-Malak, A. M. *Appl. Surf. Sci.* **2004,** *236*, 175.
33. Dileep Kumar Yadav; Maiti, B.; Quraishi, M. A. *Corros. Sci.* **2010,** *52*, 3586.
34. Quraishi, M. A.; Rawat, J.; Ajmal, M. *J. Appl. Electrochem.* **2000,** *30*, 745.